

1 **Enhancement of the North Atlantic CO<sub>2</sub> sink by Arctic Waters**

2 Jon Olafsson<sup>1</sup>, Solveig R. Olafsdottir<sup>2</sup>, Taro Takahashi<sup>3,5</sup>, Magnus Danielsen<sup>2</sup> and Thorarinn  
3 S. Arnarson<sup>4,5</sup>

4  
5 <sup>1</sup> Institute of Earth Sciences, Sturlugata 7 Askja, University of Iceland, IS 101 Reykjavik,  
6 Iceland. [jo@hi.is](mailto:jo@hi.is)

7 <sup>2</sup> Marine and Freshwater Research Institute, Fornubúðir 5, IS 220 Hafnafjörður, Iceland

8 <sup>3</sup> Lamont-Doherty Earth Observatory of Columbia University, Palisades, NY 10964, U.S.A.

9 <sup>4</sup> National Energy Authority, Grensásvegur 9, IS 108 Reykjavík, Iceland

10 <sup>5</sup> Deceased

11  
12 **Abstract**

13 The North Atlantic north of 50°N is one of the most intense ocean sink areas for atmospheric  
14 CO<sub>2</sub> considering the flux per unit area, 0.27 Pg-C yr<sup>-1</sup>, equivalent to -2.5 mol C m<sup>-2</sup> yr<sup>-1</sup>. The  
15 Northwest Atlantic Ocean is a region with high anthropogenic carbon inventories. This is on  
16 account of processes which sustain CO<sub>2</sub> air-sea fluxes, in particular strong seasonal winds,  
17 ocean heat loss, deep convective mixing and CO<sub>2</sub> drawdown by primary production. The  
18 region is in the northern limb of the Global Thermohaline Circulation, a path for the long term  
19 deep sea sequestration of carbon dioxide. The surface water masses in the North Atlantic are  
20 of contrasting origins and character, on the one hand the northward flowing North Atlantic  
21 Drift, a Gulf Stream offspring, on the other hand southward moving cold low salinity Polar  
22 and Arctic Waters with signatures from Arctic freshwater sources. We have studied by  
23 observations, the CO<sub>2</sub> air-sea flux of the relevant water masses in the vicinity of Iceland in all  
24 seasons and in different years. Here we show that the highest ocean CO<sub>2</sub> influx is to the  
25 Arctic and Polar waters, respectively, -3.8±0.4 mol C m<sup>-2</sup> yr<sup>-1</sup> and -4.4±0.3 mol C m<sup>-2</sup> yr<sup>-1</sup>.  
26 These waters are CO<sub>2</sub> undersaturated in all seasons. The Atlantic Water is a weak or neutral  
27 sink, near CO<sub>2</sub> saturation, after poleward drift from subtropical latitudes. These characteristics  
28 of the three water masses are confirmed by data from observations covering 30 years. We  
29 relate the Polar and Arctic Water persistent undersaturation and CO<sub>2</sub> influx to the excess  
30 alkalinity derived from Arctic sources. Carbonate chemistry equilibrium calculations indicate  
31 clearly that the excess alkalinity may support at least 0.058 Pg-C yr<sup>-1</sup>, a significant portion of  
32 the North Atlantic CO<sub>2</sub> sink. The Arctic contribution to the North Atlantic CO<sub>2</sub> sink which we  
33 reveal is previously unrecognized. However, we point out that there are gaps and conflicts in  
34 the knowledge about the Arctic alkalinity and carbonate budgets and that future trends in the  
35 North Atlantic CO<sub>2</sub> sink are connected to developments in the rapidly warming and changing

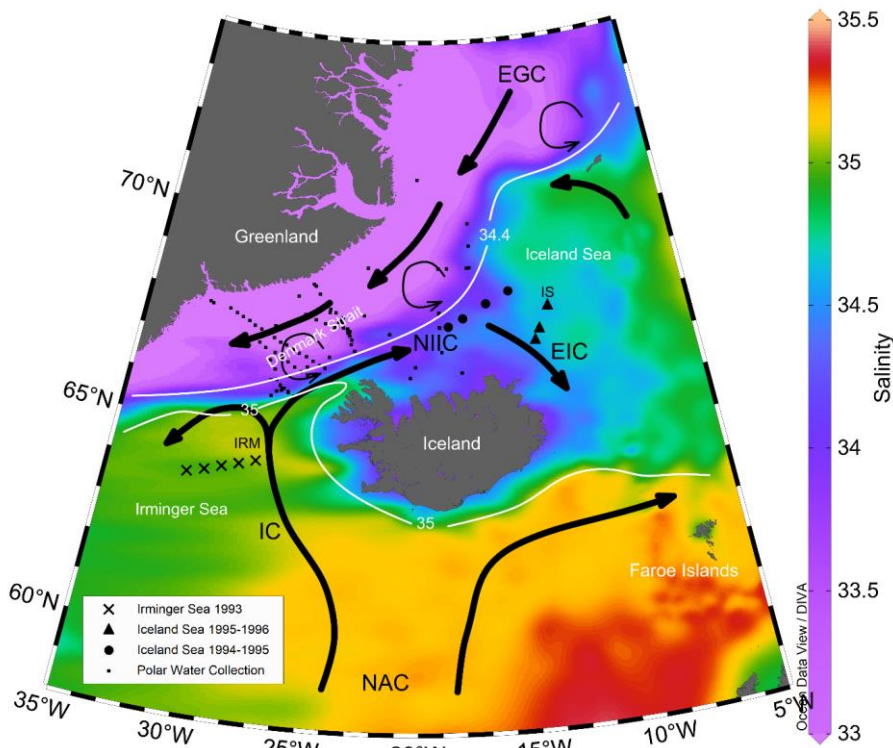
36 Arctic. The results we present need to be taken into consideration for the question: Will the  
37 North Atlantic continue to absorb CO<sub>2</sub> in the future as it has in the past?

38

## 39 **1 Introduction**

40 The oceans take up about a quarter of the annual anthropogenic CO<sub>2</sub> emissions (Friedlingstein  
41 et al., 2019). This may even be an underestimate (Watson et al., 2020). The North Atlantic  
42 north of 50°N is one of the most intense ocean sink areas for atmospheric CO<sub>2</sub> considering the  
43 flux per unit area (Takahashi et al., 2009). The reasons are strong winds and large natural  
44 partial pressure differences,  $\Delta p\text{CO}_2 = (p\text{CO}_{2\text{sw}} - p\text{CO}_{2\text{a}})$ , between the atmosphere and the  
45 surface ocean. The  $\Delta p\text{CO}_2$  in seawater is a measure of the escaping tendency of CO<sub>2</sub> from  
46 seawater to the overlying air. The  $\Delta p\text{CO}_2$  is proportional to the concentration of  
47 undissociated CO<sub>2</sub> molecules, [CO<sub>2</sub>]aq, which constitutes about 1 % of the total CO<sub>2</sub>  
48 dissolved in seawater (the remainders being about 90-95 % as [HCO<sub>3</sub><sup>-</sup>] and 4-9 % as [CO<sub>3</sub><sup>2-</sup>]).  
49 The seawater  $p\text{CO}_2$  depends sensitively on temperature and the TCO<sub>2</sub>/Alk ratio, the relative  
50 concentrations of total CO<sub>2</sub> species dissolved in seawater (TCO<sub>2</sub> = [CO<sub>2</sub>]aq + [HCO<sub>3</sub><sup>-</sup>] +  
51 [CO<sub>3</sub><sup>2-</sup>]) and the alkalinity, Alk, which reflects the ionic balance in seawater. Large  $\Delta p\text{CO}_2$   
52 has been attributed to, a) a cooling effect on the CO<sub>2</sub> solubility in the poleward flowing  
53 Atlantic Water, b) an efficient biological drawdown of  $p\text{CO}_2$  in nutrient rich subpolar waters  
54 and c) high wind speeds over these low  $p\text{CO}_2$  waters (Takahashi et al., 2002). Evaluations of  
55  $\Delta p\text{CO}_2$  based on observation and models have indicated that the Atlantic north of 50°N and  
56 northward into the Arctic takes up as much as 0.27 Pg-C yr<sup>-1</sup>, equivalent to -2.5 mol C m<sup>-2</sup> yr<sup>-1</sup>  
57 (Takahashi et al., 2009; Schuster et al., 2013; Landschützer et al., 2013; Mikaloff Fletcher et al.,  
58 2006). The North Atlantic is a relatively well observed region of the ocean (Takahashi et al.,  
59 2009; Bakker et al., 2016; Reverdin et al., 2018). Nevertheless, estimates of long term trends  
60 for the North Atlantic CO<sub>2</sub> sink due to changes in either  $\Delta p\text{CO}_2$  or wind strength are  
61 conflicting, particularly the Atlantic Water dominated regions (Schuster et al.,  
62 2013; Landschützer et al., 2013; Wanninkhof et al., 2013). The drivers of seasonal flux  
63 variations are considered inadequately understood (Schuster et al., 2013) and a mechanistic  
64 understanding of high latitude CO<sub>2</sub> sinks is regarded incomplete (McKinley et al., 2017). It  
65 has been common to many large scale flux evaluations, modelled or from observations, that  
66 they are based on regions defined by geographical borders, latitude and longitude, e.g.  
67 between 49°N and 76°N for the high latitude Sub Polar North Atlantic (Takahashi et al.,  
68 2009; Schuster et al., 2013). A more realistic approach is to define biogeographical regions,

69 biomes (Fay and McKinley, 2014). The influence of oceanographic property differences  
 70 within this region on CO<sub>2</sub> fluxes has generally not been apparent, primarily due to Arctic  
 71 latitude data limitations. The ability of current generation Earth System Models to predict  
 72 trends in North Atlantic CO<sub>2</sub> has recently been questioned and suggested that their  
 73 inadequacies may be caused by biased alkalinity in the simulated background biogeochemical  
 74 state (Lebehot et al., 2019).



75  
 76 **Figure 1. Mean July to September surface salinity in the vicinity of Iceland.** The  $S=35$   
 77 isohaline marks the boundary between northward flowing Atlantic Water and southward  
 78 flowing cold Arctic Water and low salinity Polar Water. Stations in Irminger Sea marked X  
 79 and stations in Iceland Sea marked ● for 1994-1995 and ▲ for 1995-1996 observations.  
 80 Collection of Polar Water stations 1983-2012 marked ■. IRM and IS mark the location of time  
 81 series stations. NAC: North Atlantic Current, IC: Irminger Current, NIIC: North Iceland  
 82 Irminger Current, EIC: East Icelandic Current, EGC: East Greenland Current. Map based

83 *on the NISE dataset (Nilsen et al., 2008) and drawn using the Ocean Data View program*  
84 *(Schlitzer, 2018).*

85  
86 The high latitude North Atlantic Ocean in the vicinity of Iceland, is a region of contrasting  
87 surface properties (Fig. 1). The northward flowing North Atlantic Current carries relatively  
88 warm and saline Atlantic Water, derived from the Gulf Stream, as far as the Nordic Seas and  
89 the Arctic Ocean north of Svalbard. The Irminger Current branch carries Atlantic Water to  
90 south and west Iceland and a small branch, the North Icelandic Irminger Current that  
91 transports 1 Sv ( $1 \text{ Sv} = 10^6 \text{ m}^3 \text{ s}^{-1}$ ), reaches the Iceland Sea (Stefánsson, 1962; Våge et al.,  
92 2011). The temperature and salinity properties of the Atlantic Water are known to change  
93 with atmospheric forcing and with freshening events (Dickson et al., 1988; Hátún et al.,  
94 2005; Holliday et al., 2020). The rapid East Greenland Current (EGC) (Håvik et al., 2017)  
95 flows southward from the Arctic to the North Atlantic, carrying Polar Water cold and with  
96 low salinity,  $S < 34.4$ , due to ice melt and a portion of the large freshwater input to the Arctic  
97 from rivers that contribute about 11% of the global riverine discharge (Sutherland et al.,  
98 2009; McClelland et al., 2012). In between these extremes there are large areas of the  
99 Greenland and Iceland Seas that contain predominantly the intermediate, Arctic Water which  
100 is a product of heat loss and freshwater export from the EGC (Fig. 1) (Våge et al., 2015). The  
101 north- and southward flowing currents are separated by the Arctic Front outlined in Figure 1  
102 by the salinity=35 contour generally oriented SW-NE. Deep water formation in the high  
103 latitude North Atlantic produces cold dense waters which, together with a similar product in  
104 the Labrador Sea, are source waters for the Global Thermohaline Circulation linking the  
105 regional air-sea  $\text{CO}_2$  flux to a route for the long term deep ocean sequestration of  
106 anthropogenic  $\text{CO}_2$  (Broecker, 1991). Downstream from the Polar Water and Arctic Water  
107 southward flows is the subpolar North Atlantic with high water column inventories of  
108 anthropogenic carbon (Khatiwala et al., 2013; Gruber et al., 2019). The high anthropogenic  
109  $\text{CO}_2$  regions have been attributed to the combined effects of the solubility and biology gas  
110 exchange pumps on the  $\text{CO}_2$  fluxes (Takahashi et al., 2002). The region of our study  
111 affects large scale ocean-atmosphere  $\text{CO}_2$  exchange processes in the North Atlantic.  
112 Here we evaluate regional, seasonal and interannual air-sea carbon dioxide fluxes for the main  
113 surface waters characteristic of this region (Fig. 1). We base this work on extensive  
114 observations which cover regional water masses, all seasons and include different states of the  
115 North Atlantic Oscillation, NAO (Flatau et al., 2003). We employ two different observation  
116 approaches for flux estimates. Firstly, repeat station hydrography with emphasis on the

117 seasonal flux patterns in Atlantic Water and in Arctic Water (Fig. 1). Secondly, underway  
118 ship records of surface  $p\text{CO}_2$  where the emphasis was on the different surface water masses  
119 (Fig. 2).

120

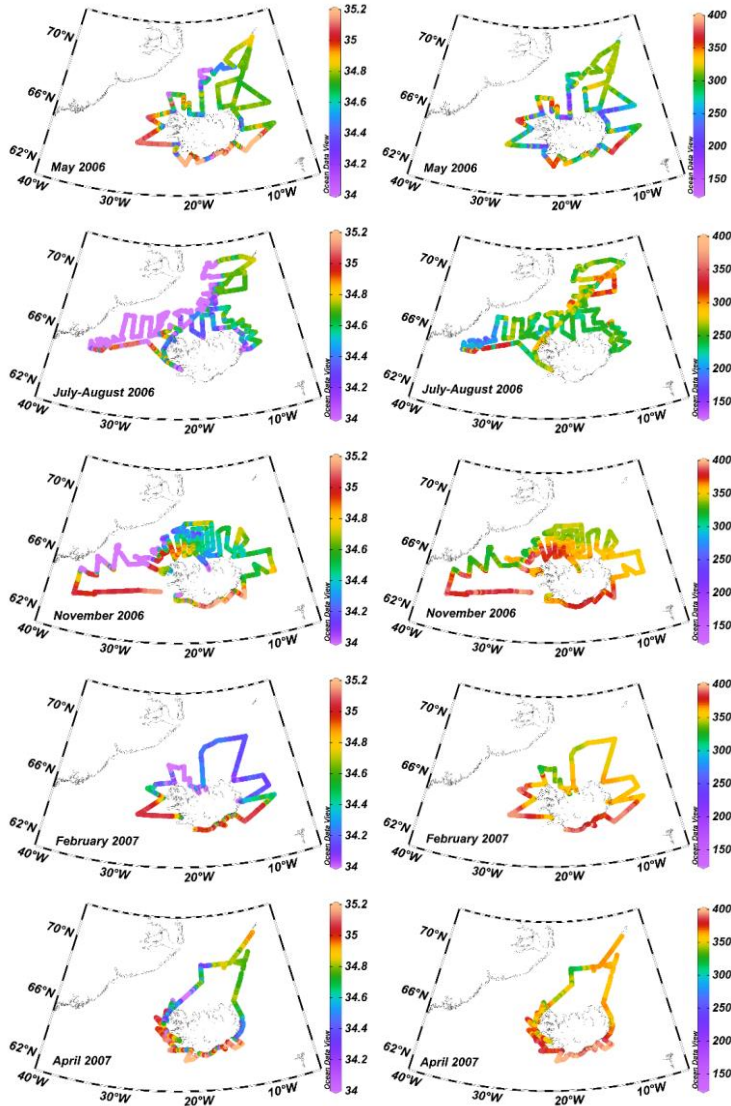
121

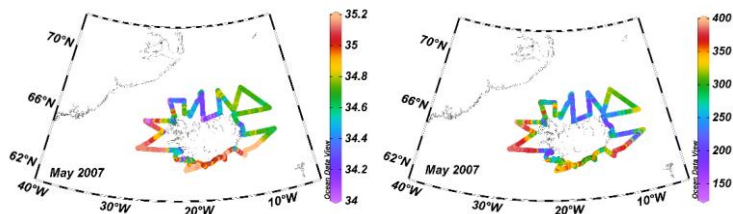
122

123

124

125





126  
127  
128  
129 **Figure 2. Cruise tracks where surface layer salinity and  $p\text{CO}_2$  were recorded**  
130 **underway.** Left sea surface salinity, right  $p\text{CO}_2\text{sw}(\mu\text{atm})$  along the cruise tracks. Maps  
131 drawn using the Ocean Data View program (Schlitzer, 2018).  
132  
133

134 We describe long term carbon chemistry characteristics of water masses in mid winter when  
135 physical forces prevail over biological processes. For the Irminger Sea and Iceland Sea from  
136 time series observations (Olafsson et al., 2010) and for the EGC Polar Water from a collection  
137 of  $p\text{CO}_2$  data assembled in the period 1983 to 2012.

## 138 2 Methods

### 139 2.1 Data acquisition

#### 140 2.1.1 Seasonal studies 1993-1996

141 Seasonal carbon chemistry variations in the relatively warm and saline ( $S>35$ ) Atlantic Water  
142 were studied 1993-1994 on 15 cruises from February 1993 to January 1994 ~~to~~with 5 stations  
143 on a 167 km long transect over the core of the Irminger Current and into the northern Irminger  
144 Sea (Fig. 1 and Tables S1 and S2). In order to close the full annual cycle, to 23 February  
145 1994 we use data from the previous year and date. In 1994-1996 the study centered on the  
146 colder and less saline Arctic Water of the Iceland Sea and was conducted on 22 cruises with  
147 sampling dates from 11 Feb 1994 to 12 Feb 1996  
148

149  
150  
151 ~~two years~~. In 1994 on 4 stations on a 168 km long transect into the Iceland Sea Gyre and in  
152 1995 on 3 stations across the East Icelandic Current (Fig. 1 and Tables S1 and S3 in the  
153 supplement). On each cruise the station work was completed in 1-2 days. For both regions,  
154 the timing of cruises was with the period of the phytoplankton spring bloom in mind  
155 (Takahashi et al., 1993). The work was conducted on vessels operated by the Marine  
156 Research Institute (MRI) in Reykjavik, Iceland, R/V Bjarni Seamundsson and R/V Arni

157 Fridriksson. Three times in 1994 a fishing vessel M/V Solrun, was hired. In August 1994 the  
158 stations were completed on the Norwegian vessel R/V Johann Hjort.  
159 Discrete surface layer, 1m, 5m and 10m,  $p\text{CO}_2$  samples were collected into 500 ml volumetric  
160 flasks and total dissolved inorganic carbon samples,  $\text{TCO}_2$ , into 250 ml flasks from water  
161 bottles on a Rosette and Sea Bird 911 CTD instruments. The  $p\text{CO}_2$  samples were preserved  
162 with mercuric chloride and analysed ashore by equilibration at 4°C with a gas of known  $\text{CO}_2$   
163 concentration followed by gas chromatography with a flame ionization detector. The  
164 instrument was calibrated with  $\text{N}_2$  reference gas and 3 standards, 197.85 ppm, 362.6 ppm and  
165 811.08 ppm, calibrated against standards certified by NOAA-CMDL at Boulder, CO, USA.  
166 ~~So were also calibrated.~~ The standards used for the underway measurements were similarly  
167 calibrated (Chipman et al., 1993). Samples for total dissolved inorganic carbon,  $\text{TCO}_2$ , were  
168 similarly preserved with mercuric chloride and analysed by coulometry ashore. Quality  
169 assurance and sample storage experiments indicated an overall precision of the discrete  
170 sample  $p\text{CO}_2$  determinations better than  $\pm 2 \mu\text{atm}$  and of the  $\text{TCO}_2$  determinations  $\pm 2 \mu\text{mol}$   
171  $\text{kg}^{-1}$  after 1990 but  $\pm 4 \mu\text{mol kg}^{-1}$  earlier (Olafsson et al., 2010).

172

### 173 **2.1.2 Underway $p\text{CO}_2$ records 2006-2007**

174 The underway  $p\text{CO}_2$  determinations in 2006-2007 covered areas of the East Greenland  
175 Current in and northwards from the Denmark Strait, in addition to Atlantic and Arctic Waters.  
176 The 6 cruises (Table S4) covered all seasons and all three water masses but with variable areal  
177 extensions (Fig. 2). Seawater was pumped continuously from an intake at 5 m depth at 10 L  
178  $\text{min}^{-1}$  into a shower-head equilibrator with a total volume of 30 L and a headspace of 15 L.  
179 Temperature at the inlet and salinity were measured with an SeaBird Model SBE-21  
180 thermosalinograph (Sea-Bird Electronics, Seattle, WA, USA). Underway  $p\text{CO}_2$  determinations  
181 were carried out with a system similar to the one described by Bates and coworkers (Bates et  
182 al., 1998). The mole fraction of  $\text{CO}_2$  ( $V \text{CO}_2$ ) in the headspace was determined with a Li-Cor  
183 infrared analyzer Model 6251 (Li-Cor Biosciences, Lincoln, NB, USA). The instrument was  
184 calibrated against four standards of  $\text{CO}_2$  in air certified by NOAA-CMDL at Boulder, CO,  
185 USA. and a  $\text{N}_2$  reference gas. The standards had  $\text{CO}_2$  dry air mole fractions of 122.19,  
186 253.76, 358.41 and 476.81 ppm. The  $p\text{CO}_2$  sw determinations were corrected to in-situ  
187 seawater temperatures using the equation (Takahashi et al., 1993):

$$188 \quad p\text{CO}_2 \text{ sw}(\text{in situ}) = p\text{CO}_2 \text{ sw}(\text{eq}) e^{0.0423(T_{\text{in situ}} - T_{\text{eq}})} \quad (\text{eq.1})$$

189 The precision of the underway  $p\text{CO}_2$  determinations is estimated by SOCAT better than  $\pm 5$   
190  $\mu\text{atm}$  (Bakker et al., 2016).

191

192

### 193 2.1.3 Time series data

194 We use discrete sample  $p\text{CO}_2$  and  $\text{TCO}_2$  data to calculate Total Alkalinity from the  
195 Irminger Sea and the Iceland Sea time series stations (Ólafsson, 2012, 2016).

196

### 197 2.1.4 Polar Water data collection

198 Discrete samples for carbon chemistry studies were taken on stations (N=146) in the East  
199 Greenland Current when opportunities permitted on cruises in the period 1983 to 2012. The 25  
200 m surface layer data include >400  $\text{TCO}_2$  samples and >300 pairs of  $p\text{CO}_2$  and  $\text{TCO}_2$  for  
201 calculation of carbonate system parameters. The seasonal cycle by month is evaluated from the  
202 composite data.

203

### 204 2.1.5 Carbonate chemistry calculations

205 The most desirable way for computing carbonate chemistry parameters is to use  $p\text{CO}_2$  and  
206  $\text{TCO}_2$  (Takahashi et al., 2014). We calculate Total alkalinity from discrete sample  $p\text{CO}_2$  and  
207  $\text{TCO}_2$  data pairs using the CO2SYS.xls v2.1 software (Lewis and Wallace, 1998; Pierrot et al.,  
208 2006) and select carbonic acid dissociation constants (Lueker et al., 2000), the constant for  
209  $\text{HSO}_4^-$  (Dickson, 1990) and boron concentrations (Lee et al., 2010).

210

## 211 2.2 $\text{CO}_2$ air-sea flux calculations

212 In this study, the partial pressure of carbon dioxide in seawater samples has been measured by  
213 gas-seawater equilibration methods (Ólafsson et al., 2010). The results are expressed as  $p\text{CO}_2$ .  
214 The bulk flux of the carbon dioxide across the air-sea interface is often estimated from its  
215 relationship with wind speed and sea-air partial pressure difference,  $\Delta p\text{CO}_2$ . We determine  
216 the flux (F) from  $\Delta p\text{CO}_2$  and use Eq. 2 and Eq. 3 for estimating the bulk air-sea fluxes of  $\text{CO}_2$   
217 (Takahashi et al., 2009)

$$218 F = k \cdot \alpha \cdot \Delta p\text{CO}_2 \quad (\text{Eq 2})$$

$$219 F = 0.251 U^2 (Sc/660)^{-0.5} \alpha (p\text{CO}_{2w} - p\text{CO}_{2a}) \quad (\text{Eq 3})$$

220 There  $k=0.251 U^2 (Sc/660)^{-0.5}$  is the gas transfer velocity or kinetic component of the  
221 expression (Wanninkhof, 2014),  $\alpha$  is the solubility of  $\text{CO}_2$  gas in sea water (Weiss, 1974) and  
222  $\Delta p\text{CO}_2 = (p\text{CO}_{2sw} - p\text{CO}_{2a})$ , is the partial pressure difference or thermodynamic component of  
223 the expression (Takahashi et al., 2009). For the wind speed, U, we use the CCMP-2



224 reanalysis wind product (Wanninkhof, 2014;Atlas et al., 2011;Wanninkhof and Triñanes,  
225 2017).

226 The atmospheric partial pressure values,  $p\text{CO}_2\text{ a}$ , used in the  $\Delta p\text{CO}_2$  calculations are weekly  
227 averages from the GLOBALVIEW-CO2 database for the CO2-ICE location which is at  
228 Vestmannaeyjar islands, off south Iceland (GLOBALVIEW-CO2, 2013). Mauna Loa values  
229 were used for periods where CO2-ICE data was missing, 1983-1992 and 2010-2012 (Tans  
230 and Keeling, 2019). The dry air  $V\text{ CO}_2$  mole fraction values were converted to  $\mu\text{atm}$  using  
231  $p\text{CO}_2(\mu\text{atm})= V\text{ CO}_2(P_a - P_w)$  where  $P_a$  is the barometric pressure and  $P_w$  is the equilibrium  
232 water vapour pressure (Weiss and Price, 1980).

233 For the Irminger Sea seasonal study we use 30 day running means of the squared daily wind  
234 speed for the region 63.5°N to 64.5°N and 27°W to 32°W and for the Iceland Sea seasonal  
235 study a similar wind product for the region 66.5°N to 68.5°N and 12°W to 19°W. Fluxes  
236 were calculated for the periods between cruises from interpolated  $p\text{CO}_2$  data and period mean  
237 30 day squared wind running means data. There are thus 14 flux periods covering a year for  
238 the Irminger sea and 21 flux periods covering two years in the Iceland Sea (Tables S1 and S2  
239 in the supplement). The annual fluxes were found by summation of the period fluxes (Table  
240 1).

241 For the underway cruises 2006 to 2007 we used CCMP-2 daily wind fields at 1x1 degree for  
242 the region 62°N to 72°N and 5°W to 40°W. This region was further divided into 4 sub-  
243 regions by latitude 64.9°N and longitude 20°W. Daily 30 day running means of the squared  
244 wind speed from two locations in each sub-region were extracted and their means used for  
245 flux calculations when the vessel sailed in the area. Fluxes were calculated for all  $p\text{CO}_2$  data  
246 from the 6 cruises, in total 42938 measurements.

247 The flux data from each of the 6 cruises were categorized into the three sea water types using  
248 the following criteria:

- 249 1) Atlantic Water  $S > 35$ , Arctic Water  $S: 34.4-34.9$ , Polar Water  $S < 34.4$ .
- 250 2) Seasonal salinity and temperature variations were taken into account.
- 251 3) Waters with runoff influences from Iceland were excluded using salinity and ship  
252 position data.

253 Thus a total of 33352 measurements were used, or 78% of the flux data points. The  $\text{CO}_2$   
254 fluxes in the realm of each water mass were assessed for the duration of each cruise by  
255 numerical integration. Fluxes in the 5 periods between cruises were assessed by interpolation  
256 of temperature, salinity and  $p\text{CO}_2$  for each water mass and by using period regional 30 day

Field Code Changed

Field Code Changed

257 running means of squared wind speed data. The annual flux for each water mass was assessed  
258 by summation.

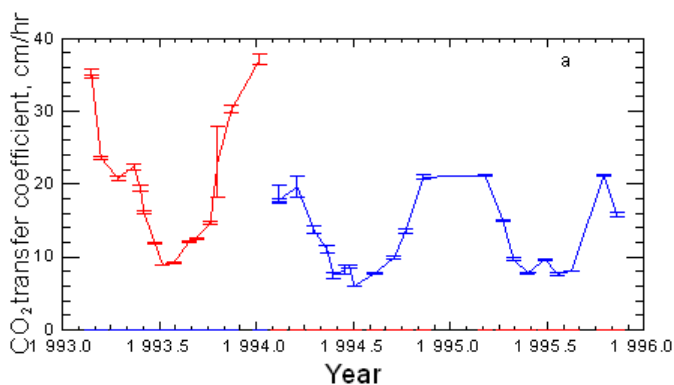
259

### 260 3 Results

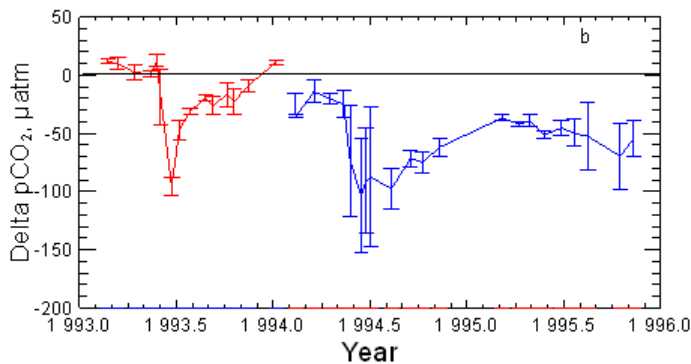
#### 261 3.1 Seasonal variations and annual CO<sub>2</sub> fluxes at regional water masses

262 The wind gas transfer coefficient reveals seasonal variations reflecting strong winds in winter  
263 when they may be stronger over the Irminger Sea than the Iceland Sea as in 1993-1994 and in  
264 1994-1995 (Fig. 3a, Fig. S1). Both the Irminger Sea and the Iceland Sea seasonal studies  
265 reveal the stongest CO<sub>2</sub> undersaturation, with negative  $\Delta p\text{CO}_2$  of about 100  $\mu\text{atm}$  in May at  
266 the time of the phytoplankton spring bloom (Fig. 3b). The undersaturation diminishes through  
267 the summer and autumn followed by a gradual return to winter conditions (Takahashi et al.,  
268 1985;Peng et al., 1987;Takahashi et al., 1993).

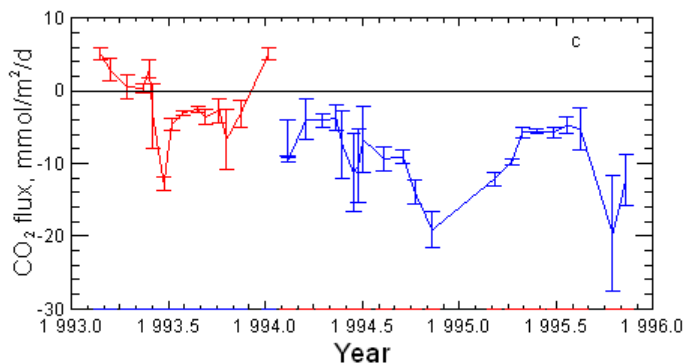
269



270



271



272 **Figure 3.** Seasonal variations in the Atlantic Water of the Irminger Sea (red) and in  
 273 the Arctic Water of the Iceland Sea (blue). The gas transfer velocity (a) reflects the seasonal  
 274 wind strength and the error bars its variations during intervals between cruises. Delta pCO<sub>2</sub>  
 275 (b) records the tendency for CO<sub>2</sub> to be transferred to the atmosphere (positive) or from the  
 276 atmosphere to the ocean (negative). The CO<sub>2</sub> flux rate (c) reveals that the Arctic Water is a  
 277 CO<sub>2</sub> sink in all seasons whereas the Atlantic Water is a source in winter and a weak sink at  
 278 other times of the year. The error bars indicate  $\pm 1$  standard deviation from the mean and  
 279 reflect the variations between the stations observed each cruise.  
 280  
 281

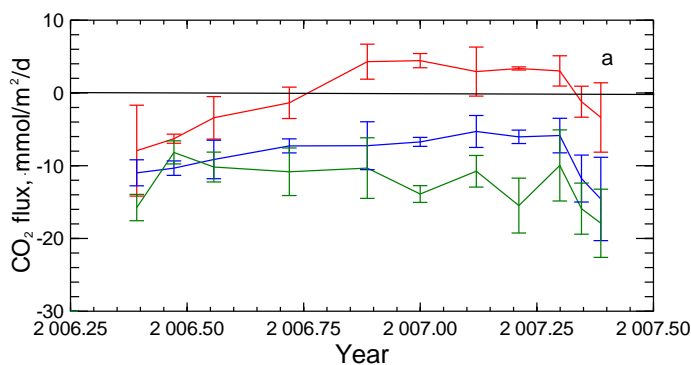
282 The CO<sub>2</sub> influx in the spring is, however, relatively small as the wind gas transfer coefficient  
 283 is then moderate (Fig. 3a). In the autumn the winds strengthen with heat loss and vertical  
 284 mixing while CO<sub>2</sub> undersaturation still persists. In mid winter, February-March, vertical  
 285 mixing brings richer CO<sub>2</sub> water to the surface of the Irminger Sea leading to supersaturation  
 286 (Ólafsson, 2003), the flux reverses and the region becomes a weak source for atmospheric  
 287 CO<sub>2</sub> (Fig. 3c).  
 288

289 **Table 1** Annual sea–air CO<sub>2</sub> fluxes (mol C m<sup>-2</sup> y<sup>-1</sup>) in the three water masses.

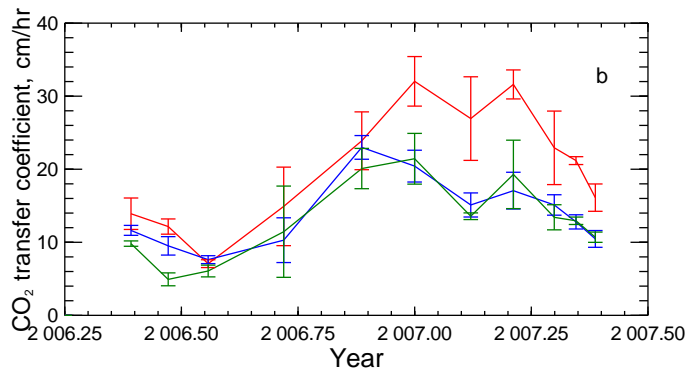
Water masses and evaluation methods	CO <sub>2</sub> flux mol C m <sup>-2</sup> y <sup>-1</sup>
Atlantic water, repeat stations 1993	-0.69±0.16
Atlantic water, Underway Measurements, 2006-2007	0.07 ± 0.15
Arctic water, repeat stations 1994	-3.97±0.48
Arctic water, repeat stations 1995	-3.60±0.31
Arctic water, Underway Measurements, 2006-2007	-2.84 ± 0.19
Polar water, Underway Measurements, 2006-2007	-4.44 ± 0.34

290

291 The integrated annual CO<sub>2</sub> flux shows that the Atlantic Water in the Irminger Sea was a weak  
 292 sink,  $-0.69 \pm 0.16 \text{ mol C m}^{-2} \text{ y}^{-1}$ , in 1993 (Table 1). The more extensive underway area  
 293 coverage of the Atlantic Water in 2006-2007, confirmed in essence the seasonal pattern and  
 294 indicated that the Atlantic Water was a neutral sink,  $0.07 \pm 0.15 \text{ mol C m}^{-2} \text{ y}^{-1}$  for this year  
 295 (Table 1). The winter gas transfer coefficient was again significantly larger over the Atlantic  
 296 Water regions than the Arctic and Polar Waters, facilitating air-sea equilibration (Fig. 4b).  
 297 The years of the Iceland Sea observations, 1994-1996, coincided with a large transition in the  
 298 North Atlantic Oscillation (NAO) from a positive state 1994/1995 to a negative state in  
 299 1995/1996 and large scale shifts in ocean fronts (Flatau et al., 2003). Vertical density  
 300 distribution in the Iceland Sea indicated an enhanced convective activity in 1995 (Våge et al.,  
 301 2015). Cold northeasterly winds were persistent in the spring of 1995 resulting in record low  
 302 temperature anomalies for the north Iceland shelf (Ólafsson, 1999). In 1995 the spring bloom  
 303 associated undersaturation,  $\Delta p\text{CO}_2$ , was only half of that in 1994, possibly due to a weaker  
 304 stratification in May and ~~and~~ continued over the summer season (Fig.S2) (Våge et al., 2015).  
 305 As in the Irminger Sea the spring bloom associated CO<sub>2</sub> influx is small. The largest CO<sub>2</sub>  
 306 influx was in the fall and early winters of 1995 and 1996 as temperature dropped, winds  
 307 gathered strength and vertical mixing was enhanced. This compensated for the small spring  
 308 bloom in 1995 and the annual bulk fluxes 1994 and 1995 are similar and high despite very  
 309 different physical conditions (Table 1). The UWpCO<sub>2</sub> surveys had less temporal resolution  
 310 but confirmed all year undersaturation of the Arctic Water. However, the integrated annual  
 311 influx,  $-2.84 \text{ mol C m}^{-2} \text{ y}^{-1}$ , was significantly less than evaluated with repeat station data even  
 312 though the strength of the gas transfer coefficient was similar in both studies (Table 1, Figs.4a  
 313 and 4b). This may reflect the large underway area coverage compared with the repeated fixed  
 314 stations.



316



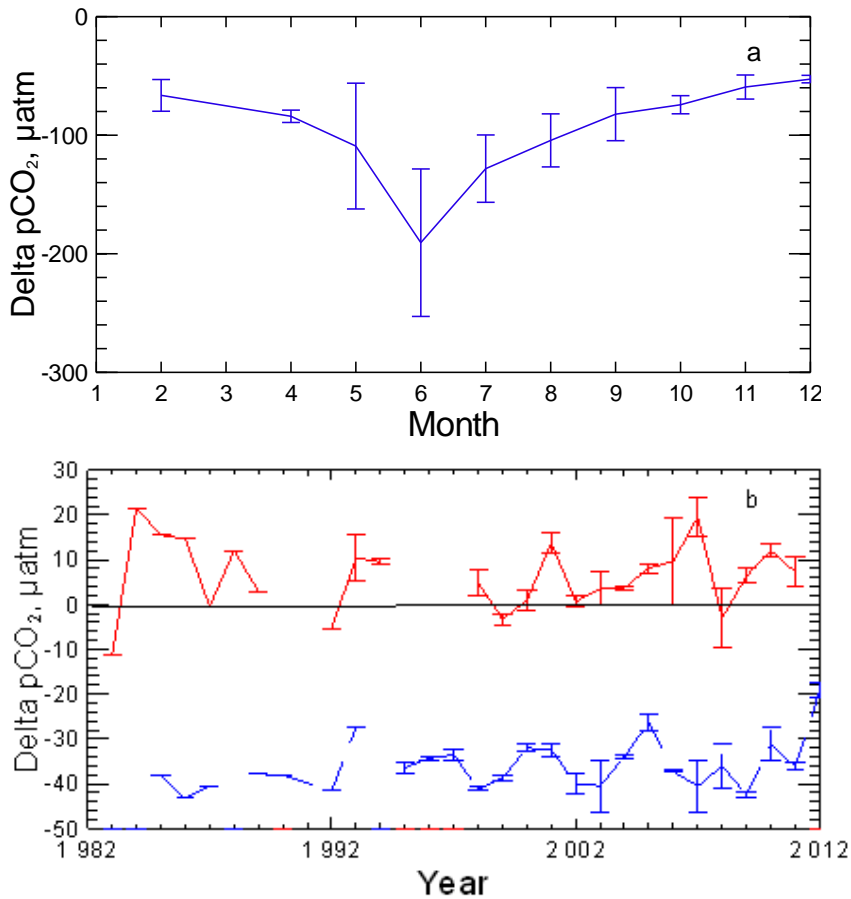
317  
 318 **Figure 4. Seasonal air-sea CO<sub>2</sub> flux variations from UWpCO<sub>2</sub> observations.**  
 319 a) Atlantic Water (red) is a weak sink in summer and neutral over the year, n=7068. Both  
 320 Arctic Water (blue) n=16874, and Polar Water (green) n=9410, are strong sinks throughout  
 321 the year. The error bars indicate ± 1 standard deviation from the mean. b) The gas transfer  
 322 coefficient for the Atlantic Water regime is significantly stronger in winter than for the Arctic  
 323 and Polar Water.

324  
 325 Ice cover in the East Greenland Current is variable and the ice edge at the seasonal minimum  
 326 has moved northward and from the Denmark Strait with decreasing Arctic sea ice (Serreze  
 327 and Meier, 2019). The Polar Water salinity ranges from 34.4 to less than 30 in summer. The  
 328 lowest salinity water freezes leading to salinity around 34 in winter. We covered the Polar  
 329 Water in all six UWpCO<sub>2</sub> surveys 2006-2007 (Fig. 2) and undersaturation characterised this  
 330 water mass in all cruises. The integrated annual influx, -4.44 mol C m<sup>-2</sup> y<sup>-1</sup> (Table 1, Fig.4),  
 331 shows the Polar Water to be the strongest CO<sub>2</sub> sink, 80 % above the estimated mean for the  
 332 Atlantic north of 50°N, -2.5 mol C m<sup>-2</sup> y<sup>-1</sup> (Takahashi et al., 2009). Further comparison with  
 333 the Takahashi climatology indicates a broad agreement with Arctic Water region NE of  
 334 Iceland with -3.5 to -4.5 mol C m<sup>-2</sup> y<sup>-1</sup> and with the Atlantic Water region S and SW of  
 335 Iceland with about -1 mol C m<sup>-2</sup> y<sup>-1</sup> (Takahashi et al., 2009).

336  
 337 **3.2 Long term ΔpCO<sub>2</sub> characteristics of the regional water masses**

338 We evaluate the long term pCO<sub>2</sub> characteristics of the three water masses from three other  
 339 data assembled over about 30 years. We use the Polar Water data collection and draft a  
 340 composite picture of seasonal ΔpCO<sub>2</sub> variations in Polar Water in and north of the Denmark  
 341 Strait (Fig.1) which confirms all year undersaturation, deep in summer, and in mid winter  
 342 when salinity raises to ~ 34, the ΔpCO<sub>2</sub> levels at about -50 μatm (Fig. 5a). Long term winter  
 343 ΔpCO<sub>2</sub> in the Irminger Sea and Iceland Sea (Figs. 1 and 5b) when biological activity is  
 344 minimal (Olafsson et al., 2009), show the Atlantic Water to be slightly supersaturated and

345 following the atmospheric  $p\text{CO}_2$  increase of  $1.80 \mu\text{atm/yr}$ , whereas the Arctic Water is  
 346 undersaturated to about  $-35 \mu\text{atm}$ . The Gulf Stream derived Atlantic Water which reaches the  
 347 northern Irminger Sea and the Nordic Seas, has had a long contact time with the atmosphere  
 348 to loose heat and reach near  $\text{CO}_2$  saturation (Takahashi et al., 2002;Olsen et al., 2006).



350  
 351 **Figure 5. Water mass decadal surface water  $p\text{CO}_2$  characteristics.** a) A composite picture of  
 352  $\Delta p\text{CO}_2$  from 146 stations with Polar Water  $p\text{CO}_2$  observations ( $n=312$ ) from the 25 m  
 353 surface layer 1983 to 2012 shows undersaturation at all times of the year. The error bars  
 354 indicate  $\pm 1$  standard deviation from the monthly means. b) Atlantic Water at the Irminger  
 355 Sea time series station (red) is generally a weak  $\text{CO}_2$  source in winter (24 winters, 52  
 356 samples), January-March, whereas winter (25 winters, 61 samples)  $\text{CO}_2$  undersaturation  
 357 persists at the Iceland Sea time series site (blue). The error bars indicate  $\pm 1$  standard  
 358 deviation from the surface layer station means.

359

360 The Polar Water in the East Greenland Current which is advected southward from the Arctic  
361 is in general characterised by low temperature and large seasonal salinity and carbonate  
362 chemistry variations. Both physical and biogeochemical processes generate the large seasonal  
363 variability but the winter observations represent the state of lowest biological activity (Fig. 6)  
364 (Table 2). The TCO<sub>2</sub> data in Table 2 are uncorrected for hydrographic variations or  
365 anthropogenic trends but the Atlantic Water is based on a short period of 10 years and the  
366 Polar Water atmospheric contact history is poorly known.

367

368 **Table 2. Mean IRM-TS Atlantic Water surface layer conditions in winter, 2001-2010**  
369 **and in Polar Water 25 m surface layer November to April 1984-2012.**

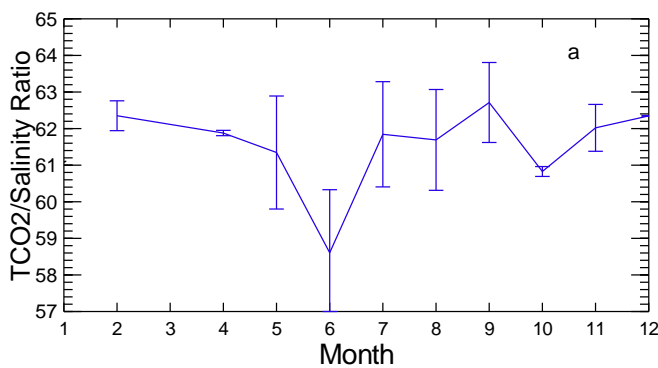
	T °C	Salinity, S	Density, $\rho$ $\text{kg m}^{-3}$	TCO <sub>2</sub> /S $\mu\text{mol kg}^{-1}$ $\text{psu}^{-1}$	ALK/S $\mu\text{mol kg}^{-1}$ $\text{psu}^{-1}$	TCO <sub>2</sub> /ALK	pCO <sub>2</sub> $\mu\text{atm}$
Atlantic Water	7.11 ± 0.36	35.13 ± 0.03	1027.507 ± 0.034	61.11 ± 0.09	65.96 ± 0.13	0.926 ± 0.002	388 ± 9
Polar Water	-0.31 ± 1.53	33.95 ± 0.33	1027.255 ± 0.244	62.16 ± 0.54	66.49 ± 0.40	0.935 ± 0.004	301 ± 11

Formatted Table

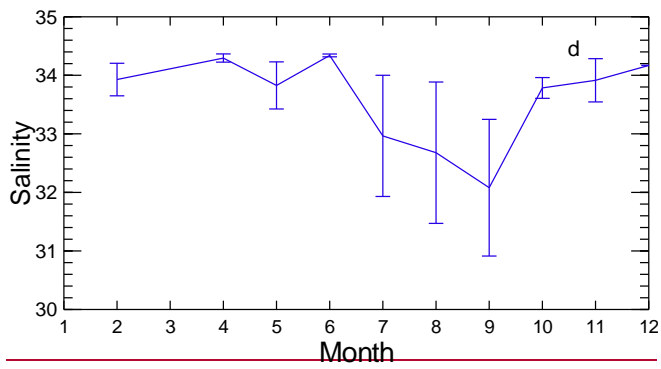
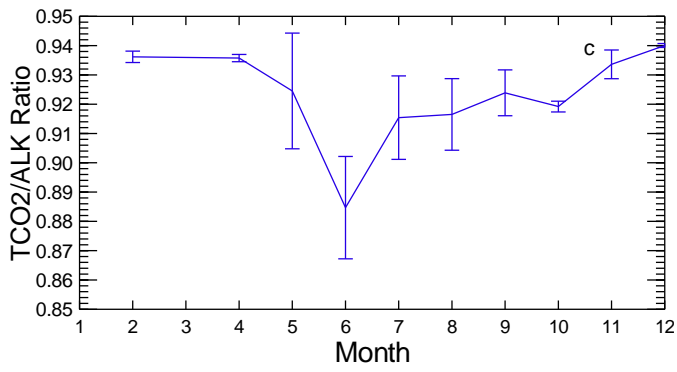
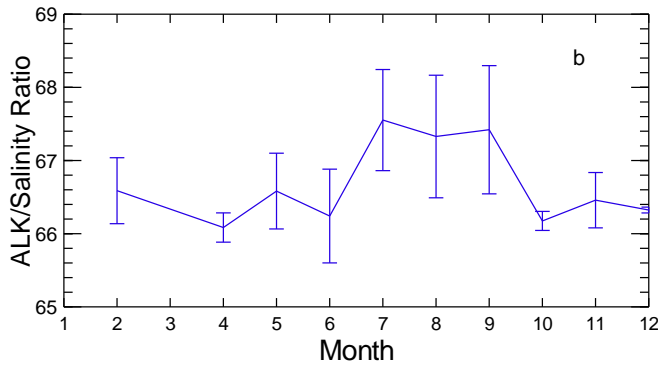
Formatted: Superscript

370

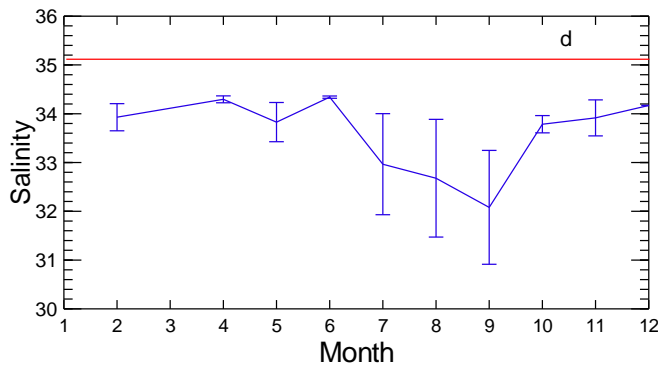
371 The winter conditions in the northward flowing Atlantic Water at the Irminger Sea time series  
372 station 2001-2010 (Table 2) are in stark contrast and with notably higher pCO<sub>2</sub> and lower  
373 TCO<sub>2</sub>/S and ALK/S ratios than the Polar Water in winter.



374







378

379 **Figure 6. Polar Water seasonal carbonate chemistry variations.** Composite Polar Water  
 380 data from the 25m surface layer. The seasonal variations in the a) Total inorganic  
 381 carbon/Salinity ratio,  $\mu\text{mol kg}^{-1} \text{psu}^{-1}$ , b) Alkalinity/Salinity ratio,  $\mu\text{mol kg}^{-1} \text{psu}^{-1}$ , and c)  
 382 Total inorganic carbon/Alkalinity ratio reflect biological carbon assimilation and inorganic  
 383 processes associated with fresh water inputs which lower the salinity d) to the annual  
 384 minimum in late summer. The red horizontal lines mark the Atlantic Water benchmarks  
 385 (Table 2).

386

387 We take the Atlantic Water in winter (Table 2) as a proxy (benchmark) for the relatively  
 388 warm and saline water advected from the North Atlantic to the Nordic Seas and the Arctic and  
 389 compare with it the carbonate chemistry seasonal variations in the southward flowing Polar  
 390 Water (Fig. 6). The ALK/S ratio for the Polar Water is higher than that for the Atlantic Water  
 391 in winter and throughout the year (Fig. 6b). The  $\text{TCO}_2/\text{S}$  ratio of the Polar Water is larger  
 392 than that of the Atlantic Water except in early summer when biological assimilation,  
 393 photosynthesis, decreases the  $\text{TCO}_2$  concentration. The  $\text{TCO}_2/\text{ALK}$  ratio falls as a  
 394 consequence (Fig. 6c) which leads to strong  $p\text{CO}_2$  undersaturation and large  $\Delta p\text{CO}_2$   
 395 (Figs 6ce and 5a). The high  $\text{TCO}_2/\text{S}$  and  $\text{ALK}/\text{S}$  ratios indicate alkalinity and carbonate  
 396 inputs as freshwater lowers the Polar Water salinity to a minimum in late summer (Fig. 6d).

397

#### 398 4 Discussion

399 The Polar Water  $\text{TCO}_2/\text{S}$  and  $\text{ALK}/\text{S}$  ratios (Table 2 and Fig. 6) indicate both alkalinity and  
 400 dissolved carbonate additions. The choice of winter ratios (Table 2) as benchmarks is solely  
 401 for the evaluation of seasonal changes in the Polar Water. Representative annual long term  
 402  $\text{TCO}_2/\text{S}$  and  $\text{ALK}/\text{S}$  means would be more realistic but are not available. Still, such a  $\text{TCO}_2/$

403 S ratio would expectedly be lower than the winter one. An assessment of the effects of the  
404 relative TCO<sub>2</sub> and ALK additions to Polar Water depends on the benchmarks chosen (Table  
405 2+).

406 The carbonate chemistry of Polar Water differs from that of open ocean waters, e.g. Atlantic  
407 Water, in having an increasingly higher alkalinity/salinity ~~and alkalinity/TCO<sub>2</sub> ratio~~ as as the  
408 salinity decreases from about S=34.4. The excess alkalinity has been attributed to the high  
409 riverine input from continents to the Arctic (Anderson et al., 2004). The flow-weighted  
410 average alkalinity of 6 major Arctic rivers, discharging  $2.245 \times 10^3 \text{ km}^3 \text{ yr}^{-1}$ , is  $1048 \text{ } \mu\text{mol kg}^{-1}$ ,  
411 however, without assessed uncertainty (Cooper et al., 2008). The river runoff into the Arctic  
412 is estimated to be about  $4.2 \times 10^3 \text{ km}^3 \text{ yr}^{-1}$ , or  $0.133 \times 10^6 \text{ m}^3 \text{ s}^{-1}$  (0.133 Sv). This is about  
413 11% of the global freshwater input to the oceans (Carmack et al., 2016). Taking the average  
414 alkalinity  $1048 \text{ } \mu\text{mol kg}^{-1}$ , the amount of alkalinity added by rivers to the Arctic and  
415 transported to the North Atlantic via the Canadian Arctic Archipelago and via the Fram Strait  
416 and further south with the Labrador and East Greenland Currents, would be  $4.4 \times 10^{12} \text{ mol yr}^{-1}$   
417 (Supplement). Cooper et al. (2008) reported on riverine alkalinity but not on associated  
418 inorganic carbonate. A recent assessment of Polar Water boron concentrations indicates  
419 insignificant borate contribution with Arctic rivers (Olafsson et al., 2020). The riverine  
420 alkalinity may primarily be attributed to carbonate alkalinity,  $\text{CA}=[\text{HCO}_3^-]+2[\text{CO}_3^{2-}]$ . The  
421 potential of the added alkalinity to reduce  $p\text{CO}_2$  of seawater would depend on its excess over  
422 TCO<sub>2</sub>.

423 Linear alkalinity-salinity relationships observed in the Arctic Ocean and the Nordic Seas and  
424 their extrapolated intercepts to S=0, have indicated freshwater sources with alkalinity  $1412$   
425  $\mu\text{mol kg}^{-1}$  (Anderson et al., 2004) and  $1752 \text{ } \mu\text{mol kg}^{-1}$  (Nondal et al., 2009). Climatological  
426 data from the West- Greenland, Iceland and Norwegian Seas show a high S=0 intercept of  
427  $1796 \text{ } \mu\text{mol kg}^{-1}$  but a lower one for the High Arctic north of  $80^\circ\text{N}$ ,  $1341 \text{ } \mu\text{mol kg}^{-1}$  (Takahashi  
428 et al., 2014). The climatological relationships were for Potential Alkalinity,  $\text{PA}=\text{TA} + \text{NO}_3^-$ ,  
429 which has little influence since the nitrate concentrations are low. The intercepts may be  
430 interpreted as the mean alkalinity of fresh waters added to the Arctic by rivers and melting ice  
431 and snow. However, the above intercepts indicate considerable variability, they are also  
432 higher than the average alkalinity of Arctic rivers,  $1048 \text{ } \mu\text{mol kg}^{-1}$ . The excess alkalinity  
433 would lower the  $p\text{CO}_2$  in seawater (and increase the pH), and thus give it an increased  
434 capacity to take up CO<sub>2</sub> from the air. The thermodynamic driving force for seawater CO<sub>2</sub>  
435 uptake,  $(p\text{CO}_{2\text{sw}} - p\text{CO}_{2\text{a}})$ , would be enhanced.

436 How large is the potential effect of excess Arctic alkalinity on the CO<sub>2</sub> uptake by the Nordic  
437 Seas and the North Atlantic? We consider an estimate. Suppose that the *p*CO<sub>2</sub> in seawater  
438 was restored to the original value by absorbing CO<sub>2</sub> from the atmosphere. The carbonate  
439 equilibrium relations in seawater give that *p*CO<sub>2</sub> is unchanged if  $\Delta\text{TCO}_2 / \Delta\text{Alk} = 0.85$  Fig. S3  
440 and Supplement. This ratio of additions is nearly constant in the temperature and salinity  
441 range of the subarctic North Atlantic surface waters (*t*=5°C, *S*=35). The volume transport of  
442 Polar Water, density <1027.8 kg m<sup>-3</sup>, by the EGC has recently been estimated as 3.9 Sv (Våge  
443 et al., 2013). Taking *S*=33.0 for the mean Polar Water salinity and using Equations 6 and 7 in  
444 Nondal et al (2009), the mean Polar Water alkalinity is 2256 μmol kg<sup>-1</sup> which is 46 μmol kg<sup>-1</sup>  
445 more alkalinity than for Atlantic Water calculated at the same salinity (Nondal et al., 2009).  
446 This much excess alkalinity would lower the *p*CO<sub>2</sub> of Atlantic Water by 88 μatm and  
447 increase the pH by 0.10. Thus, the excess alkalinity advected to the North Atlantic by the  
448 EGC is 5.7 x 10<sup>12</sup> mol yr<sup>-1</sup>. Using 0.85 for the  $\Delta\text{TCO}_2 / \Delta\text{Alk}$  additions at a constant *p*CO<sub>2</sub>, we  
449 obtain that the contribution of the excess EGC alkalinity to the uptake of CO<sub>2</sub> from the  
450 atmosphere would be 34.8 x 10<sup>12</sup> mol CO<sub>2</sub> yr<sup>-1</sup>, or 0.058 Pg-C yr<sup>-1</sup>. The estimate corresponds  
451 to 21 % of the net CO<sub>2</sub> uptake of 0.27 Pg-C yr<sup>-1</sup> for the subarctic oceans north of 50 °N  
452 (Takahashi et al., 2009). We did not include in the estimate any alkalinity contribution with  
453 the considerable Canadian Arctic Archipelago Polar Water transport (Haine et al., 2015). The  
454 effect of excess alkalinity on the North Atlantic CO<sub>2</sub> uptake flux may therefore be  
455 substantially greater than our estimate. We note that the winter undersaturation levels, of -50  
456 μatm and -35 μatm observed in the Polar and Arctic Waters, respectively (Fig. 5), translate to  
457 excess alkalinity of 19 μmol kg<sup>-1</sup> and 21 μmol kg<sup>-1</sup> for further CO<sub>2</sub> influx downstream.  
458 The difference between the average measured Arctic river alkalinity and the regression based  
459 estimates of alkalinity sources suggests that other origins and processes than the rivers  
460 contribute to the Polar Water alkalinity exported with currents from the Arctic to the Atlantic  
461 Ocean. Photic layer primary production in the absence of calcification may lower the  
462 TCO<sub>2</sub>/Alk ratio and seawater *p*CO<sub>2</sub> in marginal seas (Bates, 2006), while acidification is  
463 increasing in other regions (Anderson et al., 2017; Qi et al., 2017) and projected to become  
464 extensive at the end of the century (Terhaar et al., 2020). Furthermore, the sea-ice seasonal  
465 formation and melting may affect the TCO<sub>2</sub>/Alk ratio (Grimm et al., 2016; Rysgaard et al.,  
466 2007). Efforts to reconstruct alkalinity fields and alkalinity climatology for the Arctic have  
467 however been difficult (Broullón et al., 2019).

468

469 The Arctic is complex and complex climate warming related changes are observed in the  
470 western Arctic Ocean (Ouyang et al., 2020) and expected in marine freshwater systems of the  
471 warming Arctic (Carmack et al., 2016). Not least is the ice cover and areas of multi-year ice  
472 decreasing (Serreze and Meier, 2019). River water alkalinity increases with an addition of  
473 cations derived from the chemical weathering of silicate and carbonate rocks (Berner and  
474 Berner, 1987). Accordingly, an increase in Arctic weathering rates, in response to warmer  
475 climate and increasing atmospheric CO<sub>2</sub>, could increase the river water alkalinity transported  
476 into the oceans. Such an increase would lower the *p*CO<sub>2</sub> in seawater and enhance the oceanic  
477 uptake of atmospheric CO<sub>2</sub>, providing a negative feedback mechanism to the climatic  
478 warming resulting from increased atmospheric CO<sub>2</sub>.

479

## 480 **5 Conclusions**

481 The North Atlantic region we describe has Atlantic Waters advected from southern temperate  
482 latitudes and cold lower salinity Arctic and Polar Waters carried with the East Greenland  
483 Current from the Arctic. The Atlantic Water seasonal *p*CO<sub>2</sub> variations are primarily driven by  
484 regional thermal and biological cycles but without much net annual influx of CO<sub>2</sub>. The  
485 southward flowing Arctic and Polar Waters are on the contrary strong and persistent all year  
486 CO<sub>2</sub> sinks. These waters are advected towards the sub-polar North Atlantic with high  
487 inventories of anthropogenic carbon. The TCO<sub>2</sub>/S and ALK/S Polar Water ratios are higher  
488 than those for the Atlantic Water indicating carbonate and alkalinity sources. We point here to  
489 the Polar Water and Arctic Water CO<sub>2</sub> influx and excess alkalinity as an additional  
490 unrecognized source contributing to the North Atlantic CO<sub>2</sub> sink. We also see that there are  
491 gaps and conflicts in the knowledge about the Arctic alkalinity and carbonate budgets and that  
492 future trends in the North Atlantic CO<sub>2</sub> sink are connected to developments in the rapidly  
493 warming and changing Arctic.

494

## 495 **Acknowledgements**

496 The NMR Nordic Environmental Research Programme: Carbon Cycle and Convection in the  
497 Nordic Seas, supported the Marine Research Institute (MRI), Reykjavik, repeat station study  
498 in 1993-1995. The MRI work in 2006-2008 was supported by the European Union 6th  
499 Framework Program CARBOOCEAN, EU Contract: 511176. Taro Takahashi was supported  
500 to work on the manuscript with a grant from the the US National Oceanographic and  
501 Atmospheric Administration. The CCMP-2 wind product was generously provided from  
502 Remote Sensing Systems ([www.remss.com/measurements/CCMP](http://www.remss.com/measurements/CCMP)) by Dr. Joaquin Triñanes

503 of CIMAS/AOML, Miami. We gratefully acknowledge the long term technical support from  
504 John Goddard and Tim Newberger, Lamont-Doherty Earth Observatory. We are grateful for  
505 the invaluable cooperation we have had with the crews of all vessels operated in this study  
506 and to Norwegian colleagues for providing time for station work in August 1994.

507

508

509 *Author Contributions.* J.O., T.T. and S.R.O. wrote the manuscript. J.O., Th.S.A., S.R.O. and  
510 M.D. conducted the fieldwork. J.O., T.T. S.R.O. and Th.S.A., conceived this study.

511

512 *Competing interests.* The authors declare no competing financial interests.

513

514 *Data availability.*

515 The underway  $p\text{CO}_2$  data is available at Ocean Carbon Data System (OCADS) (Takahashi et  
516 al., 2019). The Irminger Sea and Iceland Sea seasonal study data and the Polar Water  
517 collection data are stored at the Marine and Freshwater Research Institute, Reykjavik and  
518 available by request. Irminger Sea and Iceland Sea time series data for calculation of Delta  
519  $p\text{CO}_2$  in winter is at NOAA National Centers for Environmental Information (Ólafsson, 2016,  
520 2012).

521

## 522 **References**

523

524 Anderson, L. G., Jutterström, S., Kaltin, S., and Jones, E. P.: Variability in river runoff  
525 distribution in the Eurasian Basin of the Arctic Ocean, *Journal of Geophysical Research*, 109,  
526 doi:10.1029/2003JC001733, 2004.

527 Anderson, L. G., Ek, J., Ericson, Y., Humborg, C., Semiletov, I., Sundbom, M., and Ulfsbo,  
528 A.: Export of calcium carbonate corrosive waters from the East Siberian Sea, *Biogeosciences*,  
529 14, 1811-1823, 10.5194/bg-14-1811-2017, 2017.

530 Atlas, R., Hoffman, R. N., Ardizzzone, J., Leidner, S. M., Jusem, J. C., Smith, D. K., and  
531 Gombos, D.: A cross-calibrated multiplatform ocean surface wind velocity product for  
532 meteorological and oceanographic applications, *Bull. Amer. Meteor. Soc.*, 92, 157-174,  
533 10.1109/IGARSS.2008.4778804, 2011.

534 Bakker, D. C. E., Pfeil, B., Landa, C. S., Metzl, N., O'Brien, K. M., Olsen, A., Smith, K.,  
535 Cosca, C., Harasawa, S., Jones, S. D., Nakaoka, S., Nojiri, Y., Schuster, U., Steinhoff, T.,  
536 Sweeney, C., Takahashi, T., Tilbrook, B., Wada, C., Wanninkhof, R., Alin, S. R., Balestrini,  
537 C. F., Barbero, L., Bates, N. R., Bianchi, A. A., Bonou, F., Boutin, J., Bozec, Y., Burger, E.  
538 F., Cai, W. J., Castle, R. D., Chen, L., Chierici, M., Currie, K., Evans, W., Featherstone, C.,  
539 Feely, R. A., Fransson, A., Goyet, C., Greenwood, N., Gregor, L., Hankin, S., Hardman-  
540 Mountford, N. J., Harlay, J., Hauck, J., Hoppema, M., Humphreys, M. P., Hunt, C. W., Huss,  
541 B., Ibáñez, J. S. P., Johannessen, T., Keeling, R., Kitidis, V., Körtzinger, A., Kozyr, A.,  
542 Krasakopoulou, E., Kuwata, A., Landschützer, P., Lauvset, S. K., Lefèvre, N., Lo Monaco,  
543 C., Manke, A., Mathis, J. T., Merlivat, L., Millero, F. J., Monteiro, P. M. S., Munro, D. R.,

544 Murata, A., Newberger, T., Omar, A. M., Ono, T., Paterson, K., Pearce, D., Pierrot, D.,  
 545 Robbins, L. L., Saito, S., Salisbury, J., Schlitzer, R., Schneider, B., Schweitzer, R., Sieger, R.,  
 546 Skjelvan, I., Sullivan, K. F., Sutherland, S. C., Sutton, A. J., Tadokoro, K., Telszewski, M.,  
 547 Tuma, M., van Heuven, S. M. A. C., Vandemark, D., Ward, B., Watson, A. J., and Xu, S.: A  
 548 multi-decade record of high-quality fCO<sub>2</sub> data in version 3 of the Surface Ocean CO<sub>2</sub> Atlas  
 549 (SOCAT), *Earth Syst. Sci. Data*, 8, 383-413, 10.5194/essd-8-383-2016, 2016.  
 550 Bates, N. R., Takahashi, T., Chipman, D. W., and Knap, A. H.: Variability of pCO<sub>2</sub> on diel to  
 551 seasonal timescales in the Sargasso Sea near Bermuda, *Journal of Geophysical Research:*  
 552 *Oceans*, 103, 15567-15585, 10.1029/98jc00247, 1998.  
 553 Bates, N. R.: Air-sea CO<sub>2</sub> fluxes and the continental shelf pump of carbon in the Chukchi Sea  
 554 adjacent to the Arctic Ocean, *Journal of Geophysical Research: Oceans*, 111,  
 555 10.1029/2005jc003083, 2006.  
 556 Berner, E. K., and Berner, R. A.: *The Global Water Cycle, Geochemistry and Environment*,  
 557 Prentice-Hall, Englewood Cliffs, NJ, 1987.  
 558 Broecker, W. S.: The Great Ocean Conveyor, *Oceanography*, 4, 79-89, 1991.  
 559 Broullón, D., Pérez, F. F., Velo, A., Hoppema, M., Olsen, A., Takahashi, T., Key, R. M.,  
 560 Tanhua, T., González-Dávila, M., Jeansson, E., Kozyr, A., and van Heuven, S. M. A. C.: A  
 561 global monthly climatology of total alkalinity: a neural network approach, *Earth Syst. Sci.*  
 562 *Data*, 11, 1109-1127, 10.5194/essd-11-1109-2019, 2019.  
 563 Carmack, E. C., Yamamoto-Kawai, M., Haine, T. W. N., Bacon, S., Bluhm, B. A., Lique, C.,  
 564 Melling, H., Polyakov, I. V., Straneo, F., Timmermans, M.-L., and Williams, W. J.:  
 565 Freshwater and its role in the Arctic Marine System: Sources, disposition, storage, export, and  
 566 physical and biogeochemical consequences in the Arctic and global oceans, *J. Geophys. Res.*  
 567 *Biogeosci.*, 121, 675-717, doi:10.1002/2015JG003140, 2016.  
 568 Chipman, D., Marra, J., and Takahashi, T.: Primary production at 47°N and 20°W in the  
 569 North Atlantic Ocean: a comparison between the <sup>14</sup>C incubation method and the mixed layer  
 570 budget, *Deep Sea Research II*, 40, 151-169, 1993.  
 571 Cooper, L. W., McClelland, J. W., Holmes, R. M., Raymond, P. A., Gibson, J. J., C. K. Guay,  
 572 and Peterson, B. J.: Flow-weighted values of runoff tracers (δ<sup>18</sup>O, DOC, Ba, alkalinity) from  
 573 the six largest Arctic rivers, *Geophysical Research Letters*, 35, doi:10.1029/2008GL035007,  
 574 2008.  
 575 Dickson, A. G.: Standard Potential of the Reaction - AgCl(S)+1/2H<sub>2</sub>(G)=Ag(S)+HC l(Aq)  
 576 and the Standard Acidity Constant of the ion HSO<sub>4</sub><sup>-</sup> in Synthetic Sea-Water from 273.15-K to  
 577 318.15-K, *J Chem Thermodyn*, 22, 113-127, Doi 10.1016/0021-9614(90)90074-Z, 1990.  
 578 Dickson, R. P., Meincke, J., Malmberg, S. A., and Lee, A. J.: The Great salinity Anomaly in  
 579 the northern North Atlantic, *Progress in Oceanography*, 20, 103-151, 1988.  
 580 Fay, A. R., and McKinley, G. A.: Global open-ocean biomes: mean and temporal variability,  
 581 *Earth Syst. Sci. Data*, 6, 273-284, 10.5194/essd-6-273-2014, 2014.  
 582 Flatau, M. K., Talley, L., and Niiler, P. P.: The North Atlantic Oscillation, surface current  
 583 velocities, and SST changes in the subpolar North Atlantic, *Journal of Climate*, 16, 2355-  
 584 2369, 2003.  
 585 Friedlingstein, P., Jones, M. W., O'Sullivan, M., Andrew, R. M., Hauck, J., Peters, G. P.,  
 586 Peters, W., Pongratz, J., Sitch, S., Le Quééré, C., Bakker, D. C. E., Canadell, J. G., Ciais, P.,  
 587 Jackson, R. B., Anthoni, P., Barbero, L., Bastos, A., Bastrikov, V., Becker, M., Bopp, L.,  
 588 Buitenhuis, E., Chandra, N., Chevallier, F., Chini, L. P., Currie, K. I., Feely, R. A., Gehlen,  
 589 M., Gilfillan, D., Gkritzalis, T., Goll, D. S., Gruber, N., Gutekunst, S., Harris, I., Haverd, V.,  
 590 Houghton, R. A., Hurtt, G., Ilyina, T., Jain, A. K., Joetzjer, E., Kaplan, J. O., Kato, E., Klein  
 591 Goldewijk, K., Korsbakken, J. I., Landschützer, P., Lauvset, S. K., Lefèvre, N., Lenton, A.,  
 592 Lienert, S., Lombardozi, D., Marland, G., McGuire, P. C., Melton, J. R., Metzl, N., Munro,  
 593 D. R., Nabel, J. E. M. S., Nakaoka, S. I., Neill, C., Omar, A. M., Ono, T., Peregón, A., Pierrot,

594 D., Poulter, B., Rehder, G., Resplandy, L., Robertson, E., Rödenbeck, C., Séférian, R.,  
595 Schwinger, J., Smith, N., Tans, P. P., Tian, H., Tilbrook, B., Tubiello, F. N., van der Werf, G.  
596 R., Wiltshire, A. J., and Zaehle, S.: Global Carbon Budget 2019, *Earth Syst. Sci. Data*, 11,  
597 1783-1838, 10.5194/essd-11-1783-2019, 2019.

598 GLOBALVIEW-CO2: Cooperative Global Atmospheric Data Integration Project. 2013,  
599 updated annually. Multi-laboratory compilation of synchronized and gap-filled atmospheric  
600 carbon dioxide records for the period 1979-2012 obspack\_co2\_1\_GLOBALVIEW-  
601 CO2\_2013\_v1.0.4\_2013-12-23, 2013.

602 Grimm, R., Notz, D., Glud, R. N., Rysgaard, S., and Six, K. D.: Assessment of the sea-ice  
603 carbon pump: Insights from a three-dimensional ocean-sea-ice-biogeochemical model  
604 (MPIOM/HAMOCC), *Elementa: Science of the Anthropocene*, 4, doi:  
605 10.12952/journal.elementa.000136  
606 elementascience.org, 2016.

607 Gruber, N., Clement, D., Carter, B. R., Feely, R. A., van Heuven, S., Hoppema, M., Ishii, M.,  
608 Key, R. M., Kozyr, A., Lauvset, S. K., Lo Monaco, C., Mathis, J. T., Murata, A., Olsen, A.,  
609 Perez, F. F., Sabine, C. L., Tanhua, T., and Wanninkhof, R.: The oceanic sink for  
610 anthropogenic CO<sub>2</sub> from 1994 to 2007, *Science*, 363, 1193-1199, 10.1126/science.aau5153,  
611 2019.

612 Haine, T. W. N., Curry, B., Gerdes, R., Hansen, E., Karcher, M., Lee, C., Rudels, B., Spreen,  
613 G., Steur, L. d., Stewart, K. D., and Woodgate, R.: Arctic freshwater export: Status,  
614 mechanisms, and prospects, *Global and Planetary Change*, 125, 13-35, 2015.

615 Håvik, L., Pickart, R. S., Våge, K., Torres, D., Thurnherr, A. M., Beszczynska-Möller, A.,  
616 Walczowski, W., and Appen, W.-J. v.: Evolution of the East Greenland Current from Fram  
617 Strait to Denmark Strait: Synoptic measurements from summer 2012, *J. Geophys. Res.*  
618 *Oceans*, 122, 1974-1994, doi:10.1002/2016JC01222, 2017.

619 Hátún, H., Sandø, A. B., Drange, H., Hansen, B., and Valdimarsson, H.: Influence of the  
620 Atlantic Subpolar Gyre on the Thermohaline Circulation, *Science*, 309, 1841-1844, 2005.

621 Holliday, N. P., Bersch, M., Berx, B., Chafik, L., Cunningham, S., Florindo-López, C., Hátún,  
622 H., Johns, W., Josey, S. A., Larsen, K. M. H., Mulet, S., Oltmanns, M., Reverdin, G., Rossby,  
623 T., Thierry, V., Valdimarsson, H., and Yashayaev, I.: Ocean circulation causes the largest  
624 freshening event for 120 years in eastern subpolar North Atlantic, *Nature Communications*,  
625 11, 585, 10.1038/s41467-020-14474-y, 2020.

626 Khatiwala, S., Tanhua, T., Mikaloff Fletcher, S., Gerber, M., Doney, S. C., Graven, H. D.,  
627 Gruber, N., McKinley, G. A., Murata, A., Ríos, A. F., and Sabine, C. L.: Global ocean storage  
628 of anthropogenic carbon, *Biogeosciences*, 10, 2169-2191, 10.5194/bg-10-2169-2013, 2013.

629 Landschützer, P., Gruber, N., Bakker, D. C. E., Schuster, U., Nakaoka, S., Payne, M. R.,  
630 Sasse, T. P., and Zeng, J.: A neural network-based estimate of the seasonal to inter-annual  
631 variability of the Atlantic Ocean carbon sink, *Biogeosciences*, 10, 7793-7815, 10.5194/bg-10-  
632 7793-2013, 2013.

633 Lebehot, A. D., Halloran, P. R., Watson, A. J., McNeall, D., Ford, D. A., Landschützer, P.,  
634 Lauvset, S. K., and Schuster, U.: Reconciling Observation and Model Trends in North  
635 Atlantic Surface CO<sub>2</sub>, *Global Biogeochemical Cycles*, 33, 1204-1222,  
636 10.1029/2019gb006186, 2019.

637 Lee, K., Kim, T.-W., Byrne, R. H., Millero, F. J., Feely, R. A., and Liu, Y.-M.: The universal  
638 ratio of boron to chlorinity for the North Pacific and North Atlantic oceans, *Geochimica et*  
639 *Cosmochimica Acta*, 74, 1801-1811, 2010.

640 Lewis, E., and Wallace, D.: Programme developed for CO<sub>2</sub> system calculations, Carbon  
641 Dioxide Information Analysis Center, Oak Ridge National Laboratory, U.S. Department of  
642 Energy/ORN/CDIAC-105, 1998.

643 Lueker, T. J., Dickson, A. G., and Keeling, C. D.: Ocean pCO<sub>2</sub> calculated from dissolved  
644 inorganic carbon, alkalinity, and equations for K-1 and K-2: validation based on laboratory  
645 measurements of CO<sub>2</sub> in gas and seawater at equilibrium, *Marine Chemistry*, 70, 105-119,  
646 Doi 10.1016/S0304-4203(00)00022-0, 2000.

647 McClelland, J. W., Holmes, R. M., Dunton, K. H., and Macdonald, R. W.: The Arctic Ocean  
648 Estuary, *Estuaries and Coasts*, 35, 353–368, DOI 10.1007/s12237-010-9357-3, 2012.

649 McKinley, G. A., Fay, A. R., Lovenduski, N. S., and Pilcher, D. J.: Natural Variability and  
650 Anthropogenic Trends in the Ocean Carbon Sink, *Annu. Rev. Mar. Sci.*, 9, 125-150,  
651 10.1146/annurev-marine-010816-060529, 2017.

652 Mikaloff Fletcher, S. E., Gruber, N., Jacobson, A. R., Doney, S. C., Dutkiewicz, S., Gerber,  
653 M., Follows, M., Joos, F., Lindsay, K., Menemenlis, D., Mouchet, A., Iler, S. A. M.,  
654 Sarmiento, J. L., et al. (2006), and *Global Biogeochem. Cycles*, GB2002,  
655 doi:10.1029/2005GB002530.: Inverse estimates of anthropogenic CO<sub>2</sub> uptake, transport, and  
656 storage by the ocean, *Global Biogeochem. Cycles*, 20, doi:10.1029/2005GB002530, 2006.

657 Nilsen, J. E. Ø., Hátún, H., Mork, K. A., and Valdimarsson, H.: The NISE Dataset. , Faroese  
658 Fisheries Laboratory, Box 3051, Tórshavn, Faroe Islands, 2008.

659 Nondal, G., Bellerby, R., Olsen, A., Johannessen, T., and Olafsson, J.: Predicting the surface  
660 ocean CO<sub>2</sub> system in the northern North Atlantic: Implications for the use of Voluntary  
661 Observing Ships., *Limnology and Oceanography: Methods*, 7, 109-118, 2009.

662 Olafsson, J., Olafsdottir, S. R., Benoit-Cattin, A., Danielsen, M., Arnarson, T. S., and  
663 Takahashi, T.: Rate of Iceland Sea acidification from time series measurements,  
664 *Biogeosciences*, 6, 2661-2668, 2009.

665 Olafsson, J., Olafsdottir, S. R., Benoit-Cattin, A., and Takahashi, T.: The Irminger Sea and the  
666 Iceland Sea time series measurements of sea water carbon and nutrient chemistry 1983–2008,  
667 *Earth Syst. Sci. Data*, 2, 99-104, 10.5194/essd-2-99-2010, 2010.

668 Olafsson, J., Lee, K., Olafsdottir, S. R., Benoit-Cattin, A., Lee, C.-H., and Kim, M.: Boron to  
669 salinity ratios for Atlantic, Arctic and Polar Waters: A view from downstream, *Marine*  
670 *Chemistry*, 224, 103809, <https://doi.org/10.1016/j.marchem.2020.103809>, 2020.

671 Olsen, A., Omar, A. M., Bellerby, R. G. J., Johannessen, T., Ninnemann, U., Brown, K. R.,  
672 Olsson, K. A., Olafsson, J., Nondal, G., Kivimae, C., Kringstad, S., Neill, C., and Olafsdottir,  
673 S.: Magnitude and Origin of the Anthropogenic CO<sub>2</sub> Increase and <sup>13</sup>C Suess Effect in the  
674 Nordic Seas Since 1981, *Global Biogeochemical Cycles*, 20, GB3027,  
675 doi:10.1029/2005GB002669, 2006.

676 Ouyang, Z., Qi, D., Chen, L., Takahashi, T., Zhong, W., DeGrandpre, M. D., Chen, B., Gao,  
677 Z., Nishino, S., Murata, A., Sun, H., Robbins, L. L., Jin, M., and Cai, W.-J.: Sea-ice loss  
678 amplifies summertime decadal CO<sub>2</sub> increase in the western Arctic Ocean, *Nature Climate*  
679 *Change*, 10, 678-684, 10.1038/s41558-020-0784-2, 2020.

680 Ólafsson, J.: Connections between oceanic conditions off N-Iceland, Lake Mývatn  
681 temperature, regional wind direction variability and the North Atlantic Oscillation, *Rit*  
682 *Fiskideildar*, 16, 41-57, 1999.

683 Ólafsson, J.: Winter mixed layer nutrients in the Irminger and Iceland Seas, 1990-2000, *ICES*  
684 *Marine Science Symposia*, 219, 329-332, 2003.

685 Ólafsson, J.: Partial pressure (or fugacity) of carbon dioxide, dissolved inorganic carbon,  
686 temperature, salinity and other variables collected from discrete samples, profile and time  
687 series profile observations during the R/Vs Arni Fridriksson and Bjarni Saemundsson time  
688 series IcelandSea (LN6) cruises in the North Atlantic Ocean from 1985-02-22 to 2013-11-26  
689 (NCEI Accession 0100063). Information, N. N. C. f. E. (Ed.), NOAA National Centers for  
690 Environmental Information, 2012.

691 Ólafsson, J.: Partial pressure (or fugacity) of carbon dioxide, dissolved inorganic carbon,  
692 temperature, salinity and other variables collected from discrete sample and profile



693 observations using CTD, bottle and other instruments from ARNI FRIDRIKSSON and  
694 BJARNI SAEMUNDSSON in the North Atlantic Ocean from 1983-03-05 to 2013-11-13  
695 (NCEI Accession 0149098). Information, N. N. C. f. E. (Ed.), 2016.

696 Peng, T.-H., Takahashi, T., Broecker, W. S., and Ólafsson, J.: Seasonal variability of carbon  
697 dioxide, nutrients and oxygen in the northern North Atlantic surface water, *Tellus*, 39B, 439-  
698 458, 1987.

699 Pierrot, D., Lewis, E., and Wallace, D. W. R.: MS Excel Program Developed for CO2 System  
700 Calculations. ORNL/CDIAC-105a. Carbon Dioxide Information Analysis Center,  
701 doi: 10.3334/CDIAC/otg.CO2SYS\_XLS\_CDIAC105a. Oak Ridge National Laboratory, U.S.  
702 Department of Energy, Oak Ridge, Tennessee., Oak Ridge, Tennessee, 2006.

703 Qi, D., Chen, L., Chen, B., Gao, Z., Zhong, W., Feely, R. A., Anderson, L. G., Sun, H., Chen,  
704 J., Chen, M., Zhan, L., Zhang, Y., and Cai, W.-J.: Increase in acidifying water in the western  
705 Arctic Ocean, *Nature Clim. Change*, 7, 195-199, 10.1038/nclimate3228  
706 [http://www.nature.com/nclimate/journal/v7/n3/abs/nclimate3228.html#supplementary-](http://www.nature.com/nclimate/journal/v7/n3/abs/nclimate3228.html#supplementary-information)  
707 [information](http://www.nature.com/nclimate/journal/v7/n3/abs/nclimate3228.html#supplementary-information), 2017.

708 Reverdin, G., Metzl, N., Olafsdottir, S., Racapé, V., Takahashi, T., Benetti, M., Valdimarsson,  
709 H., Benoit-Cattin, A., Danielsen, M., Fin, J., Naamar, A., Pierrot, D., Sullivan, K., Bringas,  
710 F., and Goni, G.: SURATLANT: a 1993–2017 surface sampling in the central part of the  
711 North Atlantic subpolar gyre, *Earth Syst. Sci. Data*, 10, 1901-1924, 10.5194/essd-10-1901-  
712 2018, 2018.

713 Rysgaard, S., Glud, R. N., Sejr, M. K., Bendtsen, J., and Christensen, P. B.: Inorganic carbon  
714 transport during sea ice growth and decay: A carbon pump in polar seas, *Journal of*  
715 *Geophysical Research*, 112, 2007.

716 Schlitzer, R.: Ocean Data View, <http://odv.awi.de>, 2018.

717 Schuster, U., McKinley, G. A., Bates, N., Chevallier, F., Doney, S. C., Fay, A. R., González-  
718 Dávila, M., Gruber, N., Jones, S., Krijnen, J., Landschützer, P., Lefèvre, N., Manizza, M.,  
719 Mathis, J., Metzl, N., Olsen, A., Rios, A. F., Rödenbeck, C., Santana-Casiano, J. M.,  
720 Takahashi, T., Wanninkhof, R., and Watson, A. J.: An assessment of the Atlantic and Arctic  
721 sea-air CO<sub>2</sub> fluxes, 1990–2009, *Biogeosciences*, 10, 607-627, 10.5194/bg-10-607-2013,  
722 2013.

723 Serreze, M. C., and Meier, W. N.: The Arctic's sea ice cover: trends, variability, predictability,  
724 and comparisons to the Antarctic, *Annals of the New York Academy of Sciences*, 1436, 36-  
725 53, 10.1111/nyas.13856, 2019.

726 Stefánsson, U.: North Icelandic Waters, *Rit Fiskideildar*, 3, 1-269, 1962.

727 Sutherland, D. A., Pickart, R. S., Peter Jones, E., Azetsu-Scott, K., Jane Eert, A., and  
728 Ólafsson, J.: Freshwater composition of the waters off southeast Greenland and their link to  
729 the Arctic Ocean, *Journal of Geophysical Research: Oceans*, 114, 10.1029/2008jc004808,  
730 2009.

731 Takahashi, T., Ólafsson, J., Broecker, W. S., Goddard, J., Chipman, D. W., and White, J.:  
732 Seasonal variability of the carbon-nutrient chemistry in the ocean areas west and north of  
733 Iceland, *Rit Fiskideildar*, 9, 20-36, 1985.

734 Takahashi, T., Ólafsson, J., Goddard, J. G., Chipman, D. W., and Sutherland, S. C.: Seasonal  
735 variation of CO<sub>2</sub> and nutrient salts over the high latitude oceans: A comparative study, *Global*  
736 *Biogeochemical Cycles*, 7, 843-878, 1993.

737 Takahashi, T., Sutherland, S. C., Sweeney, C., Poisson, A., Metzl, N., Tilbrook, T., Bates, N.,  
738 Wanninkhof, R., Feely, R. A., Sabine, C., Olafsson, J., and Nojiri, Y.: Global sea-air CO<sub>2</sub> flux  
739 based on climatological surface ocean pCO<sub>2</sub>, and seasonal biological and temperature effects,  
740 *Deep-Sea Research II*, 49, 1601-1622, 2002.

741 Takahashi, T., Sutherland, S. C., Wanninkhof, R., Sweeney, C., Feely, R. A., Chipman, D.  
742 W., Hales, B., Friederich, G., Chavez, F., Sabine, C., Watson, A., Bakker, D. C. E., Schuster,

743 U., Metzl, N., Yoshikawa-Inoue, H., Ishii, M., Midorikawa, T., Nojiri, Y., Körtzinger, A.,  
744 Steinhoff, T., Hoppema, M., Olafsson, J., Arnarson, T. S., Tilbrook, B., Johannessen, T.,  
745 Olsen, A., Bellerby, R., Wong, C. S., Delille, B., Bates, N. R., and Baar, H. J. W. d.:  
746 Climatological mean and decadal change in surface ocean pCO<sub>2</sub>, and net sea-air CO<sub>2</sub> flux  
747 over the global oceans, *Deep-Sea Research II*, 56, 554-577, doi:10.1016/j.dsr2.2008.12.009,  
748 2009.

749 Takahashi, T., Sutherland, S. C., Chipman, D. W., Goddard, J. G., Ho, C., Newberger, T.,  
750 Sweeney, C., and Munro, D. R.: Climatological distributions of pH, pCO<sub>2</sub>, total CO<sub>2</sub>,  
751 alkalinity, and CaCO<sub>3</sub> saturation in the global surface ocean, and temporal changes at selected  
752 locations, *Marine Chemistry*, 164, 95-125, <http://dx.doi.org/10.1016/j.marchem.2014.06.004>,  
753 2014.

754 Takahashi, T., Sutherland, S. C., and Kozyr, A.: Global Ocean Surface Water Partial Pressure  
755 of CO<sub>2</sub> Database: Measurements Performed During 1957-2018 (LDEO Database Version  
756 2018) (NCEI Accession 0160492). Version 7.7. NOAA National Centers for Environmental  
757 Information. National Centers for Environmental Information, 2019.

758 Tans, P., and Keeling, R.: Mauna Loa CO<sub>2</sub> monthly mean data. NOAA/ESRL (Ed.), 2019.

759 Terhaar, J., Kwiatkowski, L., and Bopp, L.: Emergent constraint on Arctic Ocean  
760 acidification in the twenty-first century, *Nature*, 582, 379-383, 10.1038/s41586-020-2360-3,  
761 2020.

762 Våge, K., Pickart, R. S., Sarafanov, A., Knutsen, Ø., Mercier, H., Lherminier, P., van Aken,  
763 H. M., Meincke, J., Quadfasel, D., and Bacon, S.: The Irminger Gyre: Circulation,  
764 convection, and interannual variability, *Deep Sea Research Part I: Oceanographic Research*  
765 *Papers*, 58, 590-614, <https://doi.org/10.1016/j.dsr.2011.03.001>, 2011.

766 Våge, K., Pickart, R. S., Spall, M. A., Moore, G. W. K., Valdimarsson, H., Torres, D. J.,  
767 Y.Erofeeva, S., and Ø.Nilsen, J. E.: Revised circulation scheme north of the Denmark Strait,  
768 *Deep-Sea Research Part I*, 79, 20-39, 2013.

769 Våge, K., Moore, G. W. K., Jónsson, S., and Valdimarsson, H.: Water mass transformation in  
770 the Iceland Sea, *Deep Sea Research Part I: Oceanographic Research Papers*, 101, 98-109,  
771 <http://dx.doi.org/10.1016/j.dsr.2015.04.001>, 2015.

772 Wanninkhof, R., Park, G. H., Takahashi, T., Sweeney, C., Feely, R., Nojiri, Y., Gruber, N.,  
773 Doney, S. C., McKinley, G. A., Lenton, A., Le Quéré, C., Heinze, C., Schwinger, J., Graven,  
774 H., and Khatiwala, S.: Global ocean carbon uptake: magnitude, variability and trends,  
775 *Biogeosciences*, 10, 1983-2000, 10.5194/bg-10-1983-2013, 2013.

776 Wanninkhof, R.: Relationship between wind speed and gas exchange over the ocean revisited,  
777 *Limnol. Oceanogr.: Methods*, 12, 351-362, DOI 10.4319/lom.2014.12.351, 2014.

778 Wanninkhof, R., and Triñanes, J.: The impact of changing wind speeds on gas transfer and its  
779 effect on global air-sea CO<sub>2</sub> fluxes, *Global Biogeochem. Cycles*, 31,  
780 doi:10.1002/2016GB005592, 2017.

781 Watson, A. J., Schuster, U., Shutler, J. D., Holding, T., Ashton, I. G. C., Landschützer, P.,  
782 Woolf, D. K., and Goddijn-Murphy, L.: Revised estimates of ocean-atmosphere CO<sub>2</sub> flux are  
783 consistent with ocean carbon inventory, *Nature Communications*, 11, 4422, 10.1038/s41467-  
784 020-18203-3, 2020.

785 Weiss, R. F.: Carbon dioxide in water and seawater: The solubility of a non-ideal gas, *Marine*  
786 *Chemistry*, 2, 203-215, 1974.

787 Weiss, R. F., and Price, B. A.: Nitrous oxide solubility in water and seawater, *Marine*  
788 *Chemistry*, 8, 347-359, [https://doi.org/10.1016/0304-4203\(80\)90024-9](https://doi.org/10.1016/0304-4203(80)90024-9), 1980.

789